

## **9. Linking Perception and Neurophysiology for Motion Pattern Processing: The Computational Power of Inhibitory Connections in Cortex**

Scott A. Beardsley<sup>1</sup> and Lucia M. Vaina<sup>1,2</sup>

<sup>1</sup>Brain and Vision Research Laboratory, Department of Biomedical Engineering  
Boston University, Boston, MA, USA

<sup>2</sup>Department of Neurology  
Harvard Medical School, Boston, MA, USA

### **1 INTRODUCTION**

The motion of the visual scene across the retina, termed optic flow (Gibson, 1950), contains a wealth of information about our dynamic relationship within the environment. Perceptual information regarding heading, time to contact, object motion and object segmentation can all be recovered to various degrees by analyzing the complex motion components of optic flow; for review see (Andersen, 1997, Lappe, et al., 1999). While the usefulness of such information for visually guided actions and navigation is clear, the complex neural mechanisms underlying its processing and extraction remain, for the most part, poorly understood.

As our understanding of the ecological importance of visual motion processing has increased over the last 40 years, so to has research into the perceptual mechanisms and cortical areas where optic flow processing may occur (Andersen, et al., 2000; Bremmer, et al., 2000; Duffy, 2000; Lappe, 2000; van den Berg, 2000); for review see (Vaina, 1998). Studies of the anatomical and physiological pathways in cortex have identified a coarse hierarchy of visual motion processing in which the primary visual cortex (V1) and adjacent visual areas, such as V2 and V3, send afferent projections to motion sensitive cells in the middle temporal (MT) cortex. From MT, cells in turn project to later visual motion areas including the medial superior temporal (MST) cortex and ventral intraparietal (VIP) cortex among others (Boussaoud, et al., 1990; DeYoe & Van Essen, 1988; Felleman & Van Essen,

1991; Maunsell & Van Essen, 1983; Van Essen & Maunsell, 1983). Within this coarse hierarchy, neurons exhibit a progressive increase in receptive field size and in their ability to encode more complex forms of visual information that facilitates the ability of visual motion areas to deal more directly with the complexity of the visual scene. Understanding the computational structures that underlie this progressive increase in information complexity and their relationship to our perception of the visual scene has been a primary goal of visual motion research and motivates much of the work presented here.

A current challenge in computational neuroscience is to elucidate the architecture of the cortical circuits for sensory processing and their effective role in mediating behavior. In the visual motion system, biologically constrained computational models are playing an increasingly important role in this endeavor by providing an explanatory substrate linking psychophysical performance and the visual motion properties of single cells.

Early in the visual motion pathway, research examining the neural structures within cortical areas such as V1 and MT has begun to probe the computational and functional role of neural connectivity between and within cortical regions (Carandini & Ringach, 1997; Chey, et al., 1998; Grossberg & Williamson, 2001; Koechlin, et al., 1999; Lund, et al., 1993; Malach, et al., 1997; Stemmler, et al., 1995; Teich & Qian, 2002). Recently, neural models based on the motion properties of these areas have been developed to examine the link between neural structures and perceptual performance on psychophysical tasks (Chey et al., 1998; Grossberg & Williamson, 2001; Koechlin et al., 1999).

In the work presented here, we apply a similar methodology to examine the structure and function of optic flow-based processing of the wide-field motion patterns encountered during self-motion. By combining human perceptual performance with biologically constrained neural models our aim is to elucidate the neural structures and computational mechanisms associated with optic flow processing of the visual scene. Specifically what neural structures within visual cortex are sufficient to encode and process the perceptually relevant motion patterns typically encountered during self-motion through the environment?

## 1.1 Visual Motion Processing in Cortex

Given the wide variety of visually perceived motions we experience as we move through the world, one might expect that the visual system should contain specialized detectors sensitive to the motion components (e.g. radial, circular, planar, etc.) associated with optic flow. Human psychophysical studies support this form of specialization. Perceptual performance in tasks

examining motion pattern detection and discrimination indicate the existence of specialized detectors sensitive to radial, circular, and planar motion patterns across a wide range of psychophysical techniques (Burr, et al., 1998; Freeman & Harris, 1992; Meese & Harris, 2001ab, 2002; Morrone, et al., 1995, 1999; Regan & Beverley, 1978, 1979; Snowden & Milne, 1996, 1997; Te Pas, et al., 1996). Perceptually, these motion pattern mechanisms have been shown to integrate local motions along complex trajectories to obtain global motion percepts over wide visual fields (Burr et al., 1998; Morrone et al., 1999).

### **1.1.1 Motion Pattern Processing**

Neurophysiological studies in non-human primates support the existence of such mechanisms and, together with anatomical studies, indicate a coarse visual motion hierarchy that begins in V1 and extends into posterior parietal cortex (Boussaoud et al., 1990; DeYoe & Van Essen, 1988; Felleman & Van Essen, 1991; Maunsell & Van Essen, 1983; Van Essen & Maunsell, 1983). Within posterior parietal cortex several cortical areas have been identified, including the dorsal division of MST (MSTd), VIP and area 7a, whose neurons exhibit preferred responses to motion pattern stimuli and contain qualitatively similar visual motion properties (Duffy & Wurtz, 1991a,b, 1995, 1997b; Graziano, et al., 1994; Schaafsma & Duysens, 1996; Siegel & Read, 1997; Tanaka, et al., 1989). In light of these similarities and given the relative abundance of motion pattern studies in MSTd we focus our subsequent discussion of the physiology on this region with the understanding that the underlying computational mechanisms and visual motion properties are not necessarily unique to this area.

Single cell studies in MSTd have identified cells that respond over large regions of the visual field ( $\sim 60^\circ$ ) and exhibit preferred responses to simple motion pattern components of optic flow characterized by coherent radial, circular, and planar motions (Duffy & Wurtz, 1991a,b, 1995, 1997b; Geesaman & Andersen, 1996; Graziano et al., 1994; Lagae, et al., 1994; Orban, et al., 1992; Saito, et al., 1986; Tanaka et al., 1989, 1989). The distribution of preferred motion patterns represented within MSTd spans a continuum in the stimulus space formed by radial, circular, and spiral motions that is biased in favor of expanding motions (Geesaman & Andersen, 1996; Graziano et al., 1994). Moreover, many cells in this area also respond to planar motions, suggesting a more extensive set of preferred motions that includes the four planar directions of motion (up/down, left/right) (Duffy & Wurtz, 1991a,b, 1997b).

Within this multi-dimensional plano-radial-circular space, cells respond across a wide range of stimulus speeds and exhibit speed tuning profiles best

characterized by their filtering properties (i.e., low-pass, linear, high-pass), (Duffy & Wurtz, 1997a; Orban, et al., 1995). The preferred pattern responses of these neurons are scale and position invariant to small and moderate variations in the stimulus size, location of the center-of-motion (COM), and the visual cues conveying the motion (Geesaman & Andersen, 1996; Graziano et al., 1994; Tanaka et al., 1989). For larger variations and with tests using non-optimal stimuli, cell responses degrade continuously (Duffy & Wurtz, 1995; Graziano et al., 1994). This sensitivity to the global speed and motion pattern information contained within optic flow has led to speculation that cells in MSTd could be used to encode flow based heading through the visual scene.

Combined neurophysiological and psychophysical studies in the MT/MST complex provide indirect support for such a representation, suggesting a strong link between the patterns of neural activity and motion based perceptual performance. Microstimulation of local neural clusters has been shown to reliably bias perceptual judgments in favor of the stimulated neural cluster's preferred visual motion properties (Britten & van Wezel, 1998; Celebrini & Newsome, 1995; Salzman, et al., 1990, 1992). Analyses of psychophysical performance versus single cell responses support these findings and indicate a correlation between the intensity of a cell's response and the corresponding perceptual judgment (Britten, et al., 1992, 1996; Celebrini & Newsome, 1994). While such studies do not necessarily imply that perception occurs within the affected visual areas *per se*, they do suggest that the motion processing on which perception is based occurs in these areas.

### 1.1.2 Neural Structures within Cortical Areas

In early visual motion areas, such as the primary visual cortex (V1) and MT, single cell studies have identified a variety of intrinsic neural structures (Gilbert, et al., 1996; Gilbert & Wiesel, 1985, 1989; Gilbert, 1983, 1985, 1992; Grinvald, et al., 1986; Kisvarday, et al., 1997; Lund et al., 1993; Malach et al., 1997; McGuire, et al., 1991; Ts'o, et al., 1986). Extensive modeling of the local horizontal connections inherent in these structures, both in V1 (Ben-Yishai, et al., 1995; Stemmler et al., 1995; Worgotter, et al., 1991) and MT (Koechlin et al., 1999; Liu & Hulle, 1998), suggest the existence of complex interconnected architectures whose most basic connections can impart considerable computational power to simulated neural populations. Combined psychophysical and computational studies support these findings and further suggest that horizontal connections may play a significant role in encoding the visual motion properties associated with various psychophysical tasks (Adini, et al., 1997; Chey et al., 1998; Koechlin et al., 1999; Nowlan & Sejnowski, 1995; Stemmler et al., 1995). As the importance of such local

interactions has become clearer, attention has begun to focus on their likely structure and function in higher visual areas as well (Amir, et al., 1993; Edelman, 1996; Miikkulainen & Sirosh, 1996; Sakai & Miyashita, 1991; Taylor & Alavi, 1996; Wiskott & von der Malsburg, 1996).

## 1.2 Neural Coding of Visual Information

In the cortex, the interpretation of psychophysical and physiological data within a common neural framework is dependent on how the information is represented; for review see (deCharms & Zador, 2000). Although precise temporal codes are capable of transmitting large amounts of information between individual neurons, there is good evidence that cortical neurons represent information using a coarse population code of redundant units (Shadlen & Newsome, 1998, 1994; Softky, 1995; Softky & Koch, 1993).

Indirect support for information transfer via populations of noisy cortical units has come from computational studies across a wide range of processing modalities including motor planning for reaching (Georgopoulos, et al., 1986, 1988; Lukashin & Georgopoulos, 1993, 1994; Lukashin, et al., 1996; Salinas & Abbott, 1994, 1995), orientation discrimination, and motion direction discrimination (Sundareswaran & Vaina, 1996; Vaina, et al., 1995; Zemel, et al., 1998; Zohary, 1992). In each case, the sensory information encoded across neural populations has been shown to be computationally sufficient to extract perceptually useful information from the underlying neural representation. Theoretical studies support these empirical results, demonstrating near optimal encoding of perceptually relevant stimulus properties for a variety of population coding techniques (Seung & Sompolinsky, 1993; Snippe, 1996).

While there is wide spread support for population codes in biological systems, optimal methods for decoding the neural information remain unclear. A variety of decoding techniques have been proposed including Bayesian inference (Foldiak, 1993; Oram, et al., 1998), population vector analysis (Seung & Sompolinsky, 1993), maximum likelihood (Pouget, et al., 1998), center of mass (Snippe, 1996), and probability density estimation (Sanger, 1996; Zemel et al., 1998). However, the computational efficiency and biological plausibility of these methods are often at odds with one another, preventing general acceptance for any one technique.

### 1.3 Computational Models of Motion Pattern Processing

The use of theoretical models and computer simulations in conjunction with other experimental modalities provides a powerful approach that can be used to probe the types of neural structures that may exist in the brain and their role in mediating perception. Biologically constrained models can, for example, be used to establish whether the hypothesized neural structures are computationally sufficient to account for the experimental results derived from psychophysical and neurophysiological studies. More importantly, the assumptions built into these models (both implicit and explicit) often provide predictions regarding the underlying computational mechanisms that can, in turn, be used to guide experimental research.

The existence of qualitative similarities between the visual motion properties observed in MT and MST and the computational mechanisms believed to underlie visual motion perception has motivated the development of a wide range of biologically constrained models intended to link perception, neural structure, and function within a common computational framework. While some of these models have been developed to quantify the characteristics of motion pattern tuning and their emergent properties (Beardsley & Vaina, 1998; Beardsley, et al., 2003; Pitts, et al., 1997; Wang, 1995, 1996; Zhang, et al., 1993), others have focused on identifying the computational mechanisms sufficient to extract perceptually meaningful motion attributes, particularly those associated with estimates of self-motion (Grossberg, et al., 1999; Hatsopoulos & Warren, 1991; Lappe & Rauschecker, 1993, 1995; Lappe et al., 1996; Perrone & Stone, 1994, 1998; Royden, 1997; Zemel & Sejnowski, 1998). For example, using a winner-take-all template model of self-motion estimation, Perrone and Stone (1994, 1998) obtained heading estimates under gaze-stabilized conditions that were well matched to equivalent measures of human performance. Moreover, they observed visual motion properties that were consistent with cells in MSTd across a wide range of conditions, suggesting that MSTd is computationally sufficient to extract estimates of heading.

Throughout these models, neural structures that parallel the function of the visual motion pathway have been implemented to examine how the visual motion properties of individual cells develop and to quantify the computational mechanisms required to extract perceptually useful information from optic flow. Within this scope, such models have improved our understanding of visual motion processing in cortex. However, they have generally done little to address the functional role of neural connections *within* visual motion areas, such as MST and VIP, typically associated with flow specific heading and navigation tasks.

In the work outlined in this chapter we investigate the computational and functional role of simple horizontal connections *within* a population of MSTd-like units. Based on the known visual motion properties of cells within MSTd we ask what neural structures are computationally sufficient to encode human perceptual performance on a motion pattern discrimination task? Is a population of independently responsive units, indicative of a simple feed-forward pooling of local motion estimates, computationally sufficient to encode the perceptual task? Or are specific neural structures necessary to extract equivalent measures of human perceptual performance?

## 2 DISCRIMINATING PERTURBATIONS IN WIDE-FIELD MOTION PATTERNS

Much of the research examining motion pattern perception has focused on an observer's ability to detect coherent motions in the presence of a masking background motion. A variety of masking conditions, including both local random motion and conflicting global motion patterns, have been used to quantify the existence of motion pattern mechanisms (Burr et al., 1998; Freeman & Harris, 1992; Morrone et al., 1995). The qualitative similarities between these mechanisms and motion pattern sensitive cells found in MSTd of non-human primates has led to speculation that similar neural structures may exist in the human visual motion pathway. Such speculation has received support from recent functional imaging studies of motion direction and motion pattern perception that have reported significant activation in an area referred to as MT+, the human homologue of the MT/MST complex (de Jong, et al., 1994; Greenlee, 2000; Heeger, 1999; Morrone, et al., 2000; Rees, et al., 2000; Rutschmann, et al., 2000; Tootell, et al., 1995; Vaina, et al., 2000).

Using stimuli consistent with previous motion pattern experiments (Burr et al., 1998; Freeman & Harris, 1992; Morrone et al., 1995), we developed a unique psychophysical task designed to facilitate a more direct comparison between human perceptual performance and the visual motion properties in cortical areas, such as MSTd, believed to underlie the perceptual task. We hypothesize that if neural substrates similar to those reported in MSTd do play a role in motion pattern processing, then the bias for expanding motions should result in measurable and predictable artifacts in psychophysical performance that can provide additional insight into the underlying neural mechanisms.

If the human homologue of MSTd does play a significant role in motion pattern processing, then we would expect significant variations in psychophysical performance to arise as a function of the tested motion pattern and speed in ways that are correlated with the underlying visual motion

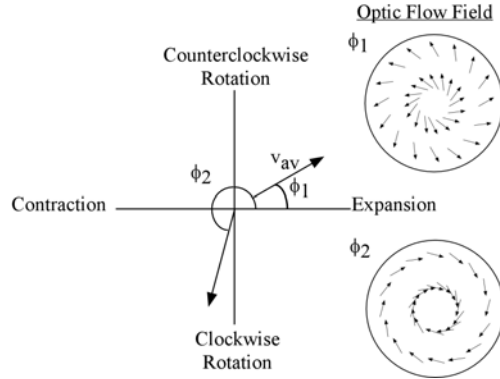


*Figure 1.* Radial, circular, and spiral motions can be represented as vectors in a 2-D stimulus space. The vector magnitude ( $v_{av}$ ) corresponds to the average dot speed across the motion field and the flow angle ( $\phi$ ) defines the type of motion pattern relative to a  $0^\circ$  baseline expansion. Off-axis regions correspond to intermediate degrees of spiral motion. [From Beardsley & Vaina, 2001; used by permission]

properties reported in MSTd. Specifically is there a preference for radially increasing speed gradients and does there exist a perceptual bias favoring the discrimination of expanding motions?

## 2.1 Methods

In a temporal two-alternative-forced-choice (2TAFC) graded motion pattern (GMP) task we measured discrimination thresholds to global changes in the patterns of complex motion (Beardsley & Vaina, 2001). Stimuli consisted of dynamic random dot displays presented in a  $24^\circ$  annular region, with the central  $4^\circ$  removed, in which each dot moved coherently from frame-to-frame such that its spatial location  $(x,y)$  in the  $n+1$  frame was given by:

$$\begin{pmatrix} x_{n+1} \\ y_{n+1} \end{pmatrix} = e^{\omega \cos \phi} \begin{pmatrix} x_n \cos(\omega \sin \phi) - y_n \sin(\omega \sin \phi) \\ x_n \sin(\omega \sin \phi) - y_n \cos(\omega \sin \phi) \end{pmatrix} \quad (1)$$

Within this representation, motion patterns could be uniquely described by their ‘flow angle’,  $\phi$ , and speed,  $\omega$ , in the 2-D stimulus space formed by cardinal (radial and circular) and spiral motions (Figure 1). Throughout the task the motion pattern remained centered in the visual display.

Prior to the start of the experiment, observers adapted for 10 sec to the background display in a darkened room. During testing observers were required to fixate a small central square and discrimination pairs of stimuli,

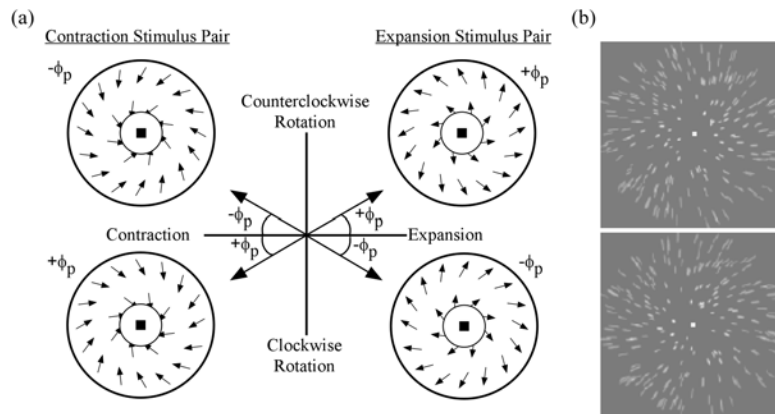


*Figure 2.* Schematic representation of the graded motion pattern (GMP) task for radial motions. All stimulus apertures were *illusory* as defined by an absence of dots. a) Pairs of stimuli were created by perturbing the flow angle ( $\phi$ ) of each 'test' motion by  $\pm\phi_p$  in the stimulus space. For the radial 'test' motions shown here, the perturbations are equivalent to the addition of a circular motion component to the 'test' motion (expansion or contraction). b) A scaled time-lapsed version of an expansion stimulus pair. [From Beardsley & Vaina, 2001; used by permission]

formed by perturbing the 'test' motion by  $\pm\phi_p$  (Figure 2), were presented following a constant stimulus paradigm ( $440\pm 40$  msec stimulus duration). To minimize the build-up of adaptation to specific motion patterns (expansion, clockwise rotation, etc.), opposing motions (e.g. expansion/contraction) were interleaved across paired presentations.

For each paired stimulus presentation observers were required to select the stimulus, via key press, containing a negative perturbation relative to the 'test' motion (Figure 2). During testing the task of discriminating negative/positive perturbations was facilitated through the presentation of radial, circular and spiral 'test' motions in separately interleaved blocks of trials. Within each block of trials observers were required to discriminate motion pattern perturbations using a conceptual simplification to the negative perturbation judgment; e.g. for radial 'test' motions select the stimulus containing a CCW motion component; for circular 'test' motions select the stimulus containing an expanding motion component, etc.

For each observer, discrimination thresholds were obtained at two average dot speeds (8.4 and  $30^\circ/\text{sec}$ ) for each of eight 'test' motions (expansion, contraction, clockwise (CW) and counterclockwise (CCW) rotation, and the four intermediate spiral motions). Within each constant stimulus session discrimination thresholds were estimated using a weighted two-parameter Weibull fit to a minimum of four perturbation levels. A  $\chi^2$  goodness-of-fit

measure with ( $\nu$ ) degrees of freedom was used to exclude data sets with poor curve fits from further analysis ( $\chi^2(\nu) < \chi_R^2(\nu)$ ;  $p < 0.1$ ), (Bevington, 1969).

## 2.2 Results

Discrimination thresholds are reported here from a subset of the observer population consisting of three experienced psychophysical observers; one of which was naïve to the purpose of the psychophysical task (Beardsley & Vaina, 2001). For each condition performance is reported as the mean and standard error averaged across 8-12 threshold estimates.

Across observers and dot speeds perceptual performance followed a distinct trend in the stimulus space with discrimination thresholds for radial motions (expansion/contraction) significantly lower than those for circular motions (CW/CCW rotation), (Figure 3). Within these sub-pairs, thresholds for radial and circular motions were well matched across observers. Figure 3 also shows that while the individual thresholds for the intermediate spiral motions were not significantly different from those for circular motions, the trends across 'test' motions were well fit by sinusoids whose period and phase were approximately  $196 \pm 10^\circ$  and  $-72 \pm 20^\circ$  respectively.

Comparable trends in performance were obtained for stimuli containing 50% flicker noise (data not shown). In this condition, dot motions were randomly assigned as 'signal' or 'noise' from frame-to-frame such that the proportion of signal dots in each frame was 50%. This resulted in a decreasing probability of uninterrupted dot motion that was structurally similar to the 2-frame motion used previously to quantify the existence of specialized motion pattern mechanisms (Burr et al., 1998; Morrone et al., 1995).

The consistency of the cyclic threshold profile in stimuli that restrict the temporal integration of individual dot motions, and simultaneously contain all directions of motion, generally argues against a primary role for local motion mechanisms in the perceptual task. While there exist a wide variety of "local" motion direction anisotropies within the psychophysical literature whose properties are reminiscent of the threshold variations observed here, (Ball & Sekuler, 1987; Coletta, et al., 1993; Edwards & Badcock, 1993; Gros, et al., 1998; Matthews & Qian, 1999; Matthews & Welch, 1997; Raymond, 1994; Zhao, et al., 1995), all predict equivalent thresholds for radial and circular motions for a set of uniformly distributed and/or spatially restricted motion direction mechanisms. Together with the need for a significant spatial integration across dispirit directions to offset the reduced temporal integration in the 50% flicker noise stimulus, this suggests the presence of a global mechanism that spatially integrates across local motions to encode more complex representations of visual motion.

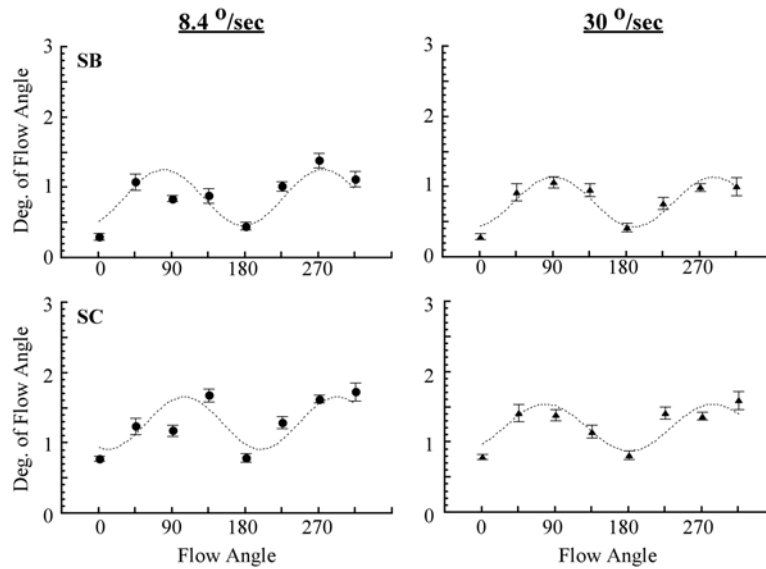


Figure 3. GMP thresholds across eight 'test' motions at two mean dot speeds (8.4 and 30°/s) for two observers (SB and SC). Performance varied continuously as a function of the 'test' motion with thresholds for radial motions ( $\phi = 0, 180$ ) significantly lower than those for circular motions ( $\phi = 90, 270$ ), ( $p < 0.001$ ;  $t(37) = 3.39$ ). Thresholds for spiral motions were not significantly different from circular motions ( $p = 0.223$ ,  $t(60) = 0.75$ ), however, the trends across 'test' motions were well fit (SB:  $r > 0.82$ , SC:  $r > 0.77$ ) by sinusoids whose period and phase were  $196 \pm 10^\circ$  and  $-72 \pm 20^\circ$  respectively.

Additional support for the role of a global motion mechanism in the perceptual task comes from a control experiment designed to assess the computational impact of the structured speed information in the stimulus. Three observers were tested using a modified set of radial and circular motions in which the radial speed gradient was removed. This condition, referred to as random speed, resulted in stimuli whose spatial distribution of dot speeds was randomized while preserving the local and global trajectory information.

In the random speed control, threshold performance increased significantly across observers, particularly for circular motions (Figure 4). Such performance suggests a measurable perceptual contribution associated with the presence of the speed gradient and is particularly interesting given the spatial symmetry implicit in the stimulus design.

Since the speed gradient was a function of the spatial distance from the stimulus center, which was itself fixed in the center of the visual display, its distribution for each 'test' motion was radially symmetric. Within this limited subset of conditions the speed gradient did not contribute computationally

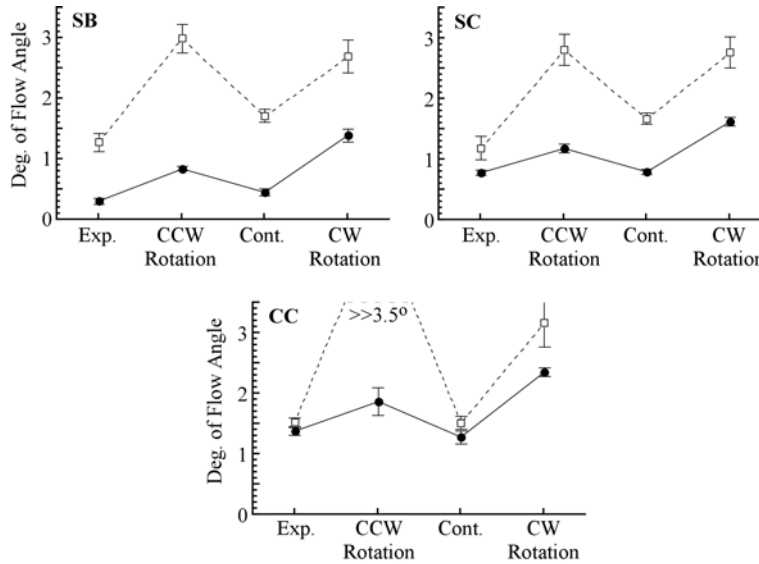


Figure 4. Radial and Circular GMP thresholds for stimuli with (filled circles) and without (open squares) a radial speed gradient (average dot speed = 8.4 deg/s). Across observers (SB, SC, and CC) thresholds for radial motions remained significantly lower than those for circular motions in the random speed condition (i.e., no speed gradient). Relative to stimuli containing speed gradients, random speed thresholds increased significantly across observers ( $p < 0.05$ ;  $t(17) = 1.91$ ), particularly for circular motions ( $p < 0.005$ ;  $t(25) = 3.31$ ).

relevant structural information to the task. However, the speed gradient did convey information regarding the integrative structure of the global motion field and as such suggests a preference in the underlying motion mechanisms for spatially structured speed information. Together with similar perceptual studies reporting the existence of wide-field motion pattern mechanisms (e.g. Burr et al., 1998; Meese & Harris 2001, 2002), these results suggest that the threshold differences observed here may be associated with variations in the computational properties across a series of specialized motion pattern mechanisms.

### 3 A COMPUTATIONAL MODEL OF MOTION PATTERN PROCESSING

#### 3.1 GMP Discrimination via a Population Code in MSTd

The similarities between the visual motion patterns used to quantify human perception and the tuning properties of cells in visual motion areas

such as MSTd and VIP suggest that such cortical regions may mediate the perceptual task. If, for example, motion pattern perception were based on a simple population code of complex motion detectors drawn from the anisotropic cell distribution reported in MSTd (Geesaman & Andersen, 1996; Graziano et al., 1994), one might expect that GMP discrimination should follow a distribution symmetric about the radial motion axis with thresholds for expansions lowest and thresholds for contractions among the highest. Within this framework, deviations in human performance from that of a simple population code could suggest the presence of horizontal connections within the population that serve to modify and refine the underlying neural representation.

To examine this hypothesis, we constructed a population of MSTd-like units whose visual motion properties were consistent with those reported in the neurophysiology (Duffy & Wurtz, 1991a,b; Geesaman & Andersen, 1996; Graziano et al., 1994; Orban et al., 1995), (Figure 5; see Beardsley & Vaina, 2001 for details). Within the model, simulations were categorized according to the underlying distribution of preferred motions represented across the population (2 reported in MSTd - Figure 5b, and a uniform control). The first distribution simulated an expansion bias in which the density of preferred motions decreased symmetrically from expansions to contractions across the motion pattern space (Graziano et al., 1994). The second distribution was similar in structure but contained a higher percentage of cells tuned to contracting motions (Geesaman & Andersen, 1996). The third distribution simulated a uniform preference for all motions and was used as a control to examine the effects of a non-homogeneous distribution on perceptual performance. Throughout the remainder of the chapter we refer to simulations containing these distributions as Unimodal, Bimodal, and Uniform respectively.

In MSTd receptive fields are large, spanning up to one-half of the visual field (Duffy & Wurtz, 1991a,b; Tanaka & Saito, 1989). For neurons preferring similar motions, the resultant overlap in visual input can introduce correlation in the neural output that varies with the relative spatial positions of the cells' receptive fields. The structure associated with such correlations implies a redundant representation of neural information that can be used to aid information extraction across populations of noisy units. To simulate this effect in the model we assumed that units had comparable receptive fields such that the responses of units with similar preferred motions were moderately correlated ( $r = [0.4, 0.8]$ ). Since the model did not explicitly contain a feed-forward layer of spatially localized inputs, we correlated neural responses by imposing a maximum preferred motion response,  $R_{max}$ , that varied as a Poisson process ( $\lambda=28$ ) for each stimulus presentation (Figure 5a).

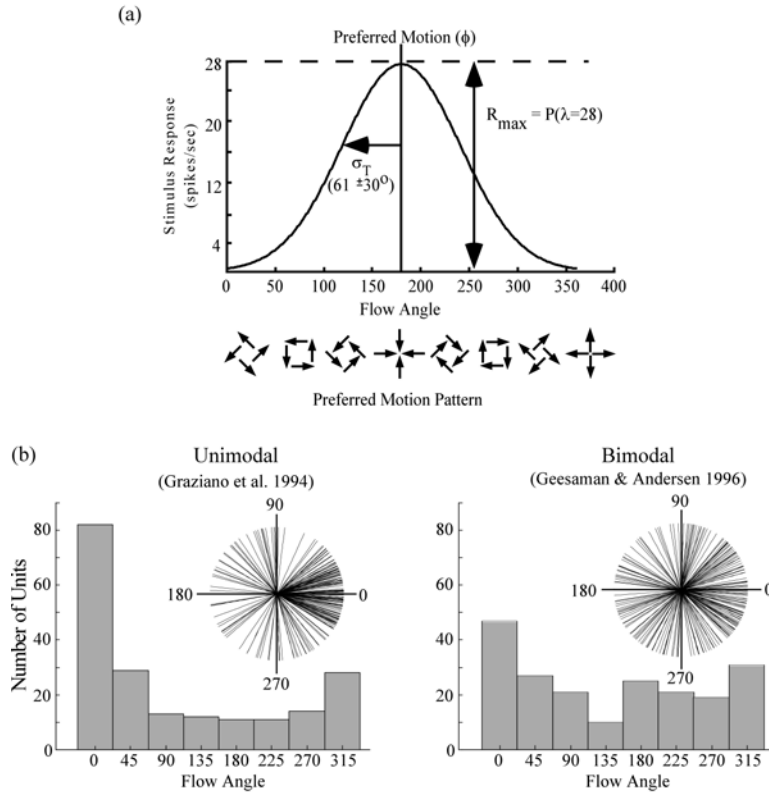


*Figure 5.* Motion pattern properties of the MSTd-like units used in the model. a) Motion pattern tuning followed a gaussian profile ( $\sigma_T = 61^\circ \pm 30^\circ$ ) in the stimulus space centered on each unit's preferred motion. The preferred motion responses,  $R_{\max}$ , varied as a Poisson process based on the reported range of firing rates in MSTd. b) The preferred motion for each unit was selected randomly from a continuous distribution consistent with one of two distributions reported in MSTd. [From Beardsley & Vaina, 2001; used by permission]

The baseline neural output of each unit ( $N_i$ ) was simulated as an uncorrelated Poisson process ( $\lambda=12$ ).

### 3.1.1 Extracting Perceptual Estimates from the Neural Code

The psychophysical task was simulated in the model using a "population vector" to represent the net motion pattern estimated in the 2-D stimulus space (Figure 1). A structural diagram of the model is shown in Figure 6. For each

stimulus, the response of the  $i^{\text{th}}$  unit was represented as the average firing rate,  $R_{av}$ , estimated from the unit's motion pattern tuning profile (Figure 5a),

$$R_{av_i} = R_{max} e^{-\frac{(\phi - \phi_i)^2}{2\sigma_i^2}} \quad (2)$$

where  $R_{max}$  is the maximum preferred stimulus response (spikes/s),  $\phi$  is the stimulus flow angle and  $\phi_i$  and  $\sigma_i$  correspond to the preferred motion and standard deviation of the  $i^{\text{th}}$  unit's tuning profile respectively. The net response,  $R_i$ , of each unit was formed by combining  $R_{av_i}$  with the baseline neural output  $N_i$ .

For each stimulus, units 'voted' for their preferred motions with a weight equal to their net firing rate. Across the population weighted responses were represented as vectors in the units' preferred motion directions and estimates of the stimulus flow angle were decoded as the "population vector" formed from the vector sum of responses across all units.

Using the population vector estimates obtained for each set of paired stimuli, the model's performance was quantified according to the negative perturbation ( $-\phi_p$ ) discrimination of flow angle outlined in the psychophysical task. As with the perceptual task, a least-squares fit to percent correct performance across constant stimulus levels was used to estimate discrimination thresholds.

### 3.2 Simulation 1: An Independent Neural Code

In the first series of simulations, we quantified GMP performance across populations of independently responding units. For each class of models (Unimodal, Bimodal, and Uniform), threshold performance was examined across five populations (100, 200, 500, 1000, and 2000 units). Both the range in thresholds and their trends across 'test' motions were compared across simulations to identify combinations of population size and preferred motion distributions that yielded quantitatively similar performance relative to the psychophysical task.

It is important to note that within this implementation the population vector does *not* provide an unbiased estimator of the stimulus flow angle ( $\phi$ ). The bias in the distribution of preferred motions (Figure 5b) introduces a corresponding bias into the vector representation that is skewed toward expanding motions. As a result, increasing populations do not yield vector representations that converge to the proper 2-D motion pattern. This makes accurate interpretation of individually decoded stimuli problematic without

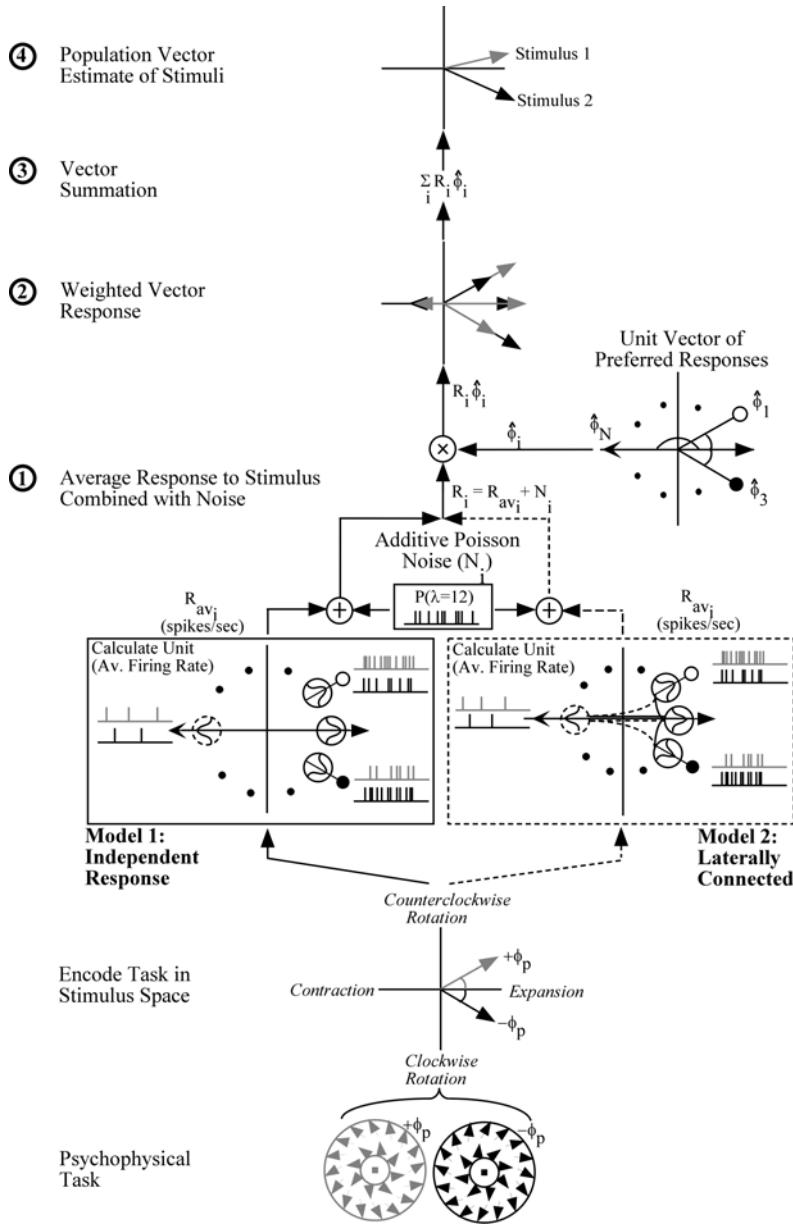


Figure 6. Schematic representation of the model structure. The psychophysical task was simulated using a vector representation of the stimuli in the 2-D motion pattern space. For each stimuli, units ‘voted’ (2) for their preferred motion with a weight equal to their net firing rate (1). Stimuli were decoded from the neural representation as the population vector formed by the vector sum of weighted responses across units (3). As in the psychophysical task, “perceptual” judgments were based on the negative perturbation ( $-\phi_p$ ) discrimination of flow angle (4). [From Beardsley & Vaina, 2001; used by permission]

*a priori* knowledge of the nonlinear transformation associated with the bias in the vector representation.

To compensate for this, the model's performance was based on the relative spatial locations *between* the pairs of motion patterns ( $\pm\phi_p$ ) presented in the 2T AFC task and not the absolute location of each decoded stimulus in the stimulus space. In this way, the population vector could assume any smooth nonlinear mapping without imposing *a priori* assumptions regarding the underlying transformation and thus was not constrained to linearly map the stimulus space onto the internal neural representation.

### 3.2.1 Simulation 1: Results

Performance varied considerably as a function of the population size and distribution of preferred motions (Figure 7). Over the psychophysical range of interest ( $\phi \pm 7^\circ$ ), discrimination thresholds for contracting motions were at chance across all Unimodal populations (100-2000 units) while thresholds for circular motions remained significantly higher than those reported in the perceptual task (Figure 7a). Across the eight 'test' motions, discrimination thresholds showed no significant improvement with increasing population size.

Discrimination thresholds for Bimodal populations were more consistent with human performance, particularly as population size increased. Contraction ( $\phi = 180^\circ$ ) thresholds for larger populations steadily decreased to those obtained for expansions ( $\phi = 0^\circ$ ), (Figure 7b), however, even with the largest populations discrimination for contracting spiral motions remained poor.

Unlike the Unimodal populations, Bimodal performance also improved asymptotically with population size. This was particularly true for contractions ( $\phi = 180^\circ$ ), which decreased by a factor of six as the size of the population was increased. While this decrease made the overall range of thresholds more comparable with human performance, Bimodal populations remained unable to accurately reproduce psychophysical thresholds in the asymptotic limit observed through 2000 units.

For simulations containing a Uniform distribution of preferred motions, the range of discrimination thresholds was consistent with human performance, however, the trend in thresholds was generally flat. What variability did occur, for small populations in particular, was due primarily to the discrete sampling of preferred motions from the uniform distribution. In subsequent simulations (not shown here), more extensive averaging reduced the observed variability, resulting in threshold profiles that were well fit by a line whose slope was near zero.

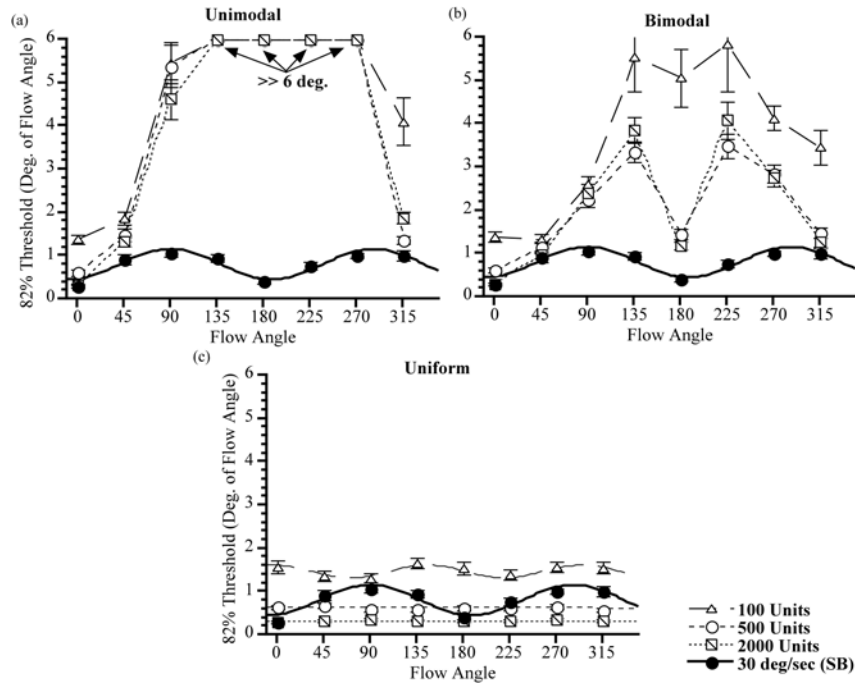


*Figure 7.* Model vs. psychophysical performance on the GMP task for three simulated populations of independently responding units. GMP thresholds ( $\pm 1$  standard error) were averaged across five independently generated populations for each population size. a) Across all populations, Unimodal thresholds were highest for contracting motions and lowest for expanding motions. b) Bimodal thresholds were more consistent with human performance (SB) particularly for moderately large populations ( $> 500$  units). Although discrimination thresholds for contracting motions ( $\phi = 180^\circ$ ) steadily decreased as the number of units increased, Bimodal populations remained unable to accurately reproduce psychophysical thresholds in the asymptotic limit observed through 2000 units. c) Across Uniform populations the range of discrimination thresholds was well-matched with human performance, however, the flat trend across motion patterns was inconsistent with the sinusoidal trend observed in the psychophysical task. [From Beardsley & Vaina, 2001; used by permission]

Examination of the pooled information within the Unimodal and Bimodal models suggests that the threshold differences resulted from the combination of background noise and the population bias for expanding motions. For non-expanding sub-populations, such as those preferring contractions, the proportion of units responsive to a non-expanding stimulus was typically a small percentage of the total population. In these cases, the population vector contained a significant amount of noise associated with the non-preferred background response. As population size increased, the non-uniform effect of

the expansion bias on the signal-to-noise ratio across the population caused discrimination thresholds to closely track the degree of preferred motion bias within each model class.

### 3.3 Simulation 2: An Interconnected Neural Structure

In a second series of simulations, we examined the computational effect of adding lateral (horizontal) connections between neural units. If the distribution of preferred motions in MSTd is in fact biased towards expansions as the neurophysiology suggests, it seems unlikely that independent estimates of the visual motion information would be sufficient to yield the perceptual profiles obtained in the psychophysical task. Instead we hypothesize that a simple fixed architecture of excitatory and/or inhibitory connections between neural units may be necessary to yield the observed psychophysical thresholds.

In this series of simulations, units were fully interconnected with fixed excitatory and/or inhibitory connections. Within this architecture, each neural response consisted of the summed output from three nonlinear sources corresponding to (a) the visual motion stimulus, (b) internal neural noise (not associated with the visual stimulus), and (c) a modulating input from other units within the population.

Across the population, connection strength varied as a function of the similarity in preferred motions between neural units. Using the flow angle representation for preferred motion patterns, excitatory connections from the  $i^{\text{th}}$  unit (with preferred motion  $\phi_i$ ) were made to units with similar preferred motions. The strength of excitation followed a Gaussian profile centered at  $\phi_i$  with a fixed standard deviation ( $\sigma_E = 30^\circ$ ) across the population. Similarly, units with anti-preferred motions received inhibitory connections whose strength followed a Gaussian profile centered at  $180+\phi_i$ . To examine the effects of inhibitory spread and connection strength in the model, the standard deviation of the inhibition profile,  $\sigma_I$ , and the level of excitatory/inhibitory activity,  $S_A$ , were considered free parameters.

#### 3.3.1 Simulation 2: Results

Within the parameter space used to define connectivity between units (i.e.,  $S_A$  and  $\sigma_I$ ), both the overall level of the GMP thresholds and their trends across ‘test’ motions varied widely. Monte Carlo simulations across the parameter space yielded regions of high correlation (with respect to the psychophysical thresholds) that were consistent across independently

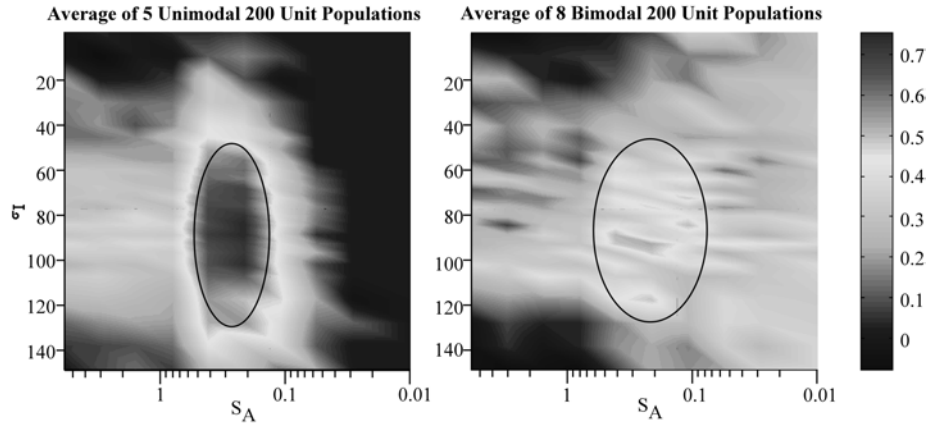


Figure 8. Correlation maps of model vs. psychophysical performance as a function of the strength of the horizontal connections,  $S_A$ , and the spread of inhibition,  $\sigma_I$ . For Unimodal/Bimodal populations the regions of interest (ROIs) denoted by the ellipses, ( $\geq 80\%$  of maximum correlation), corresponded to areas within the parameter space where model thresholds were well matched to human perceptual performance. These regions were generally robust extending over a broad range of  $\sigma_I$   $[60, 120^\circ]$  and  $S_A$   $[0.15, 0.5]$ . [From Beardsley & Vaina, 2001; used by permission]

simulated populations for both the Unimodal and Bimodal models. Typically these regions were well defined over a wide but limited range of  $\sigma_I$  and  $S_A$ . Figure 8 illustrates this result for averages of five Unimodal and eight Bimodal populations containing 200 units. In both cases the regions-of-interest (ROIs), corresponding to the areas of best correlation (80% of maximum), were generally robust, extending over a broad range of  $\sigma_I$   $[60, 120^\circ]$  and  $S_A$   $[0.15, 0.5]$ .

While the maximum level of correlation within these regions typically accounted for only a fraction of the psychophysically observed variance across motion patterns (25-50%), simulations containing 100 units indicated an increase in correlation as a function of population size. Together these results suggested that larger populations would yield regions of increasingly higher correlation, however, the computational cost precluded an exhaustive search of the parameter space for populations of more than 200 units. To offset this limitation, we confined simulations of larger populations to a set of 'optimal' parameters estimated from each ROI, (Figure 8).

Using a fixed  $\sigma_E$  ( $=30^\circ$ ), ROI center-of-mass estimates of  $[\sigma_I = 106^\circ, S_A = 1.77]$  and  $[\sigma_I = 76^\circ, S_A = 1.93]$  for 100-unit populations and of  $[\sigma_I = 88^\circ, S_A = 0.37]$  and  $[\sigma_I = 91^\circ, S_A = 0.36]$  for 200-unit populations were obtained for Unimodal and Bimodal models respectively. Given the lack of significant correlation across Uniform populations and the similarities in center-of-mass

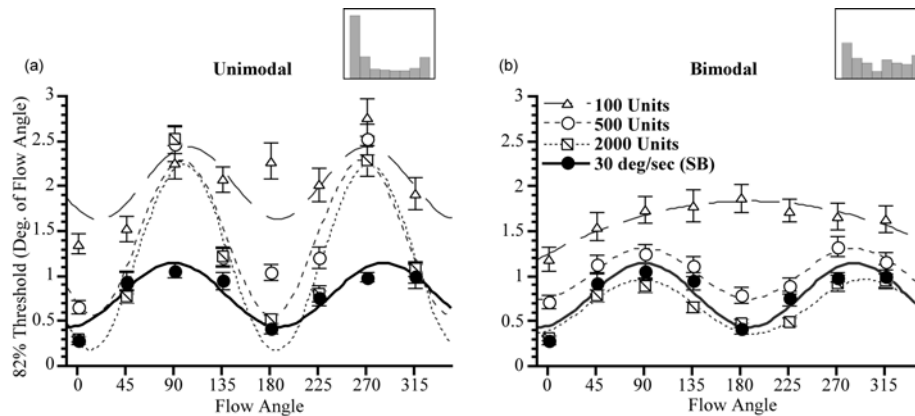


Figure 9. Model vs. psychophysical performance on the GMP task for populations containing excitatory and inhibitory horizontal connections. As the number of units increased, discrimination thresholds (averaged across five simulations) decreased to psychophysical levels and the sinusoidal trend in thresholds began to emerge for both the a) Unimodal and b) Bimodal models. Sinusoidal trends were established for as few as 500 units and were well fit ( $r > 0.9$ ) by sinusoids whose periods and phases were  $(173.7 \pm 6.9^\circ, -67.21 \pm 16.78^\circ)$  and  $(208.3 \pm 10.2^\circ, -60.68 \pm 15.74^\circ)$  for the Unimodal and Bimodal models respectively.

estimates for the Unimodal/Bimodal populations, we set  $\sigma_7$  and  $S_A$  to  $80^\circ$  and 1.5 respectively for all 100-unit populations. For larger populations the connection strength,  $S_A$ , was scaled inversely with the number of units to maintain an equivalent level of horizontal activity and facilitate a comparative analysis across populations.

Figure 9 shows the averaged threshold performance for three population sizes. The incorporation of horizontal connections between units decreased the range of discrimination thresholds to psychophysically observed levels. More importantly, as population size increased the sinusoidal trend in threshold performance emerged for both the Unimodal and Bimodal models. The threshold trends were well established for as few as 500 units and were well fit ( $r > 0.9$ ) by sinusoids whose periods and phases were consistent with the fitted psychophysical trends ( $196 \pm 10^\circ$  and  $-72 \pm 20^\circ$ ).

Unlike the Unimodal/Bimodal models, Uniform populations were not significantly affected by the presence of horizontal connections. The range of thresholds were typically well matched to those from Simulation 1 and asymptotically decreased to levels well below those of human observers for large populations (i.e., 2000 units).

Throughout the Unimodal and Bimodal simulations presented here, threshold performance decreased asymptotically with increasing population size for all 'test' motions. The decrease followed an inverse power law whose exponent varied as a function of the 'test' motion across an order of magnitude

[0.05,0.5]. For all 'test' motions the threshold slope decreased quickly with population size such that for 2000 units the change in thresholds was  $0.008^\circ$  for each 100-unit increase in the population. Together with the computational robustness to large variations in the underlying population properties (i.e. size and the distribution of preferred motions) the model's asymptotic performance makes this form of highly interconnected architecture appealing as a method for encoding visual motion information consistently across a neural population.

### 3.4 Simulation 3: Thresholding Neural Responses

In a third series of simulations we examined the effect of imposing a threshold on the unit responses contributing to the population vector. Here, sub-threshold responses were rectified to zero using a Heaviside function,  $H(T_R)$ , prior to weighting the unit's preferred motion vector

$$\begin{aligned} H(T_R) &= 0, & R_i < T_R \\ &= 1, & R_i \geq T_R \end{aligned} \quad (3)$$

where  $T_R$  is the response threshold. GMP performance was examined over a range of rectifying thresholds ( $T_R=[1,61]$  spikes/s) for each class of models. Like the previous simulations, the model's performance was correlated with the psychophysical thresholds to estimate the range of  $T_R$  over which the population code was consistent with human performance. Threshold performance was then examined as a function of population size for each of the three model classes (Unimodal, Bimodal, and Uniform) using an 'optimal'  $T_R$  selected from the composite regions of highest correlation.

#### 3.4.1 Simulation 3: Results

While the addition of horizontal connections resulted in discrimination thresholds that were in good agreement with human performance, it does not preclude other methods of noise reduction within the neural structures used to encode the visual motion information. When population vector estimates were based on a subset of thresholded ( $T_R$ ) responses within a population of unconnected units, the resulting thresholds were similar to those obtained with populations of interconnected units.

With a  $T_R$  of 35 spikes/s imposed prior to calculating the population vector, the range of discrimination thresholds decreased to psychophysically observed levels for populations containing 500 units. As with the inter-

connected populations, the sinusoidal trend in threshold performance emerged as the number of units increased. Here the cyclic trends were established for 1000 units and were well fit ( $r > 0.85$ ) by sinusoids whose periods and phases were ( $218.5 \pm 15.7^\circ$ ,  $-37.98 \pm 21.35^\circ$ ) and ( $216.9 \pm 21.9^\circ$ ,  $-42.17 \pm 30.34^\circ$ ) for Unimodal and Bimodal models respectively.

Closer examination of the response characteristics within these “thresholded” populations indicates that the proportion of units responding consistently above threshold ( $>80\%$  of the time) varied with the ‘test’ motion, from a low of 1.4% for contractions to a high of 11% for expansions (Unimodal populations). The subsequent exclusion of minimally responsive units reduced the variability of the ‘predicted’ motion pattern in a manner consistent with the presence of inhibitory horizontal connections between anti-preferred motion pattern units. As a result, for Unimodal and Bimodal models in particular, the proportion of units contributing to the population vector varied as a function of the ‘test’ motion and typically comprised only a small fraction of the total population. Such performance is generally consistent with a winner-take-all strategy of neural coding and the pre-synaptic inhibitory architecture it implies (Haykin, 1999; Hertz, et al., 1991).

### 3.5 Simulation 4: The Role of Inhibitory Connections

The development of a sinusoidal trend in GMP performance for large ( $>1000$  units) “thresholded” populations, together with the inhibitory winner-take-all structures implied by their sparse coding, suggest that similar performance could be obtained from populations containing *only* inhibitory connections. Although early simulations using small populations to search for regions of significant correlation across the  $(\sigma_i, S_A)$  parameter space were inconclusive, the inability of small “thresholded” populations in Simulation 3 to reproduce the psychophysical trend suggests that larger populations might be required. Using the ‘optimal’ structural parameters obtained previously from Simulation 2, we examined the model’s GMP performance for mutually inhibiting populations of up to 2000 units, (Figure 10).

With the inclusion of anti-preferred inhibition between units, discrimination thresholds for large populations asymptotically approached those for the interconnected excitatory/inhibitory populations (i.e. Simulation 2). As population size increased, the sinusoidal trend in thresholds emerged for both the Unimodal and Bimodal models. Typically the trend was established for as few as 1000 units and was well fit ( $r > 0.9$ ) by sinusoids whose periods and phases were consistent with the fitted psychophysical trends ( $196 \pm 10^\circ$  and  $-72 \pm 20^\circ$ ). These results are in good agreement with both the fitted psychophysical trends and the performance of the

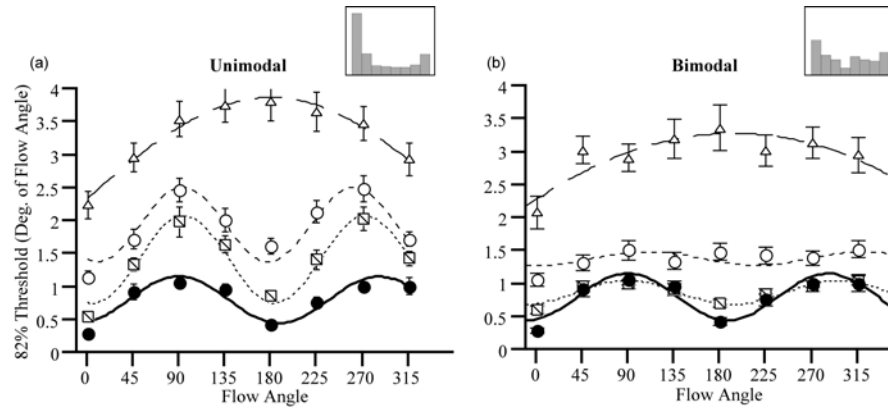


*Figure 10.* Model vs. psychophysical performance on the GMP task for populations containing only inhibitory connections. As population size increased the sinusoidal trend in thresholds emerged for both the a) Unimodal and b) Bimodal models. The trends were established for as few as 1000 units and were well fit ( $r > 0.9$ ) by sinusoids whose periods and phases were ( $178.0 \pm 6.0^\circ$ ,  $-79.48 \pm 13.93^\circ$ ) and ( $205.8 \pm 16.2^\circ$ ,  $-65.77 \pm 25.88^\circ$ ) for Unimodal and Bimodal models respectively.

interconnected excitatory/inhibitory models (Simulation 2) for moderate population sizes ( $\sim 500$  units).

As with the excitatory/inhibitory architecture simulated previously, discrimination thresholds decreased asymptotically with increases in population size. Subsequent simulations for even larger populations ( $\sim 5000$  units) showed little change in the threshold amplitudes or their trends across 'test' motions. Together with the robust encoding of motion pattern information across  $\sigma_E$  (see Beardsley & Vaina, 2001 for details), these results suggest that perceptual performance in the GMP task may be mediated primarily through signal enhancement associated with the strength and spread of inhibitory connections within a population of motion detectors selective for the simple motion pattern components of optic flow.

## 4 DISCUSSION

In the graded motion pattern (GMP) task presented here (see also Beardsley & Vaina, 2001) we have shown that human discrimination varies consistently with the pattern of complex motion over a range of thresholds ( $\phi = 0.5$ - $2^\circ$ ). For each observer, the trend across psychophysical thresholds consistently demonstrated a preference for radial motions that is qualitatively similar to the bias for expanding motions reported in MSTd. Together with

the preferences for global motion patterns reported in MSTd, these results suggest that much of the perceptual information, if not the underlying neural circuitry, involved in the discrimination of motion patterns may be represented in the human homologue to MST.

Using biologically plausible neural units we have shown that the motion information encoded across a population of MSTd neurons is sufficient to obtain discrimination thresholds consistent with human performance. Theoretically, the computations required to perform the perceptual task can be obtained by comparing the nonzero responses between pairs of motion pattern cells that adequately span the 2-D stimulus space. However, in practice neural populations are typically required to extract the desired visual motion information given the presence of neural noise not associated with the stimulus and the lack of *a priori* knowledge concerning the variability in stimulus tuning profiles across cells.

In the neural populations simulated here, the 2-D stimulus representation facilitated the choice of a "population vector" decoding strategy to extract perceptually meaningful motion pattern information. With this implementation, the bias for expanding motions reported in MSTd introduced a computational bias in the vector estimate of the flow angle ( $\phi$ ) that was skewed toward expanding motions. Under these conditions, increases in population size did not yield vector representations that converged to the proper 2-D motion pattern, making an accurate interpretation of individually decoded stimuli problematic without *a priori* knowledge of the nonlinear transformation associated with the bias.

To compensate for this, the model's performance was based on the *relative* locations between the pairs of stimuli presented in the psychophysical task and not the proper 2-D location of each decoded motion in the stimulus space. In this way, the population vector could assume any smooth nonlinear mapping without imposing *a priori* assumptions regarding the underlying transformation, and thus was not constrained to linearly map the stimulus space onto the internal neural representation.

While sufficient for the psychophysical task outlined here, this limitation in the decoding strategy restricts the model's general application to perceptual tasks consisting of single stimulus presentations. This deficiency could be overcome by using computationally more robust decoding schemes such as Bayesian inference (Oram et al., 1998) or probability density estimation (Sanger, 1996; Zemel et al., 1998) that do not require an explicit representation of the stimulus space. Within such decoding schemes the addition of inhibitory connections between units, while mathematically more complex, would seem likely to affect GMP discrimination in comparable ways by minimizing the stimulus uncertainty associated with overlapping probability distributions within a multi-dimensional representation.

Similar but less extreme conditions may also occur in models of free arm reaching (Georgopoulos et al., 1986, 1988; Lukashin & Georgopoulos, 1993, 1994; Lukashin et al., 1996) for which the monkey physiology suggests the presence of statistically significant deviations from uniformity in both motor cortex (Schwartz, et al., 1988) and parietal area 5 (Kalaska, et al., 1983). Within each of these models there has been an implicit assumption of uniformity in the neural representation that, for large populations, predicts population vector estimates will converge to the proper reaching vector representation. However if this uniformity assumption is not met, as in the model we have presented, the theoretical convergence breaks down in proportion to the degree of non-uniformity and the locations of stimulus vectors relative to the bias. Depending on the actual degree of anisotropy within cortical motor areas, asymptotic reaching errors, such as those reported by Georgopoulos et al. (1988), might in fact be artifacts associated with an underlying non-uniformity in the 3-D reaching representation.

#### **4.1 Motion Pattern Discrimination in a Population of Independently Responding Units**

Using a population of MSTd-like neural units we have demonstrated that the population vector information decoded from independently responding units *is not* computationally sufficient to extract perceptual estimates that are consistent with human performance. For anisotropic neural populations containing a strong bias for expanding motions (Unimodal and Bimodal models), large amounts of noise are introduced into the population vector estimate for non-expanding stimuli. In the extreme case of contracting motions, only 20% of the population typically responded to the stimulus. For those units that did respond significantly, the encoded signal-to-noise ratio was typically offset by a significantly larger noise contribution encoded across the sub-population of non-responsive units. This introduced considerable variability in the motion pattern estimated from the population, causing discrimination thresholds to increase.

In contrast the control simulations, containing a uniform distribution of preferred motions across the population, were able to approximate the psychophysical range of discrimination thresholds. However, they did not develop the sinusoidal trend in thresholds observed across 'test' motions. If, as we have hypothesized, the trend in threshold performance were due to a combination of neural properties (such as the distribution of preferred motion patterns) inherent to the cells underlying the perceptual task, then we would not have expected the Uniform models to deviate significantly from the flat trend obtained across all conditions.

Taken together these results suggest that a population code of independent neural responses is capable of extracting perceptual information relevant to the motion pattern task. However, the model's strong dependence on population size and the distribution of preferred motions prevent this scheme from producing the robust trends in psychophysical performance reported across observers.

## 4.2 The Computational Role of Horizontal Connections

The addition of horizontal connections that minimized neural noise within the population produced discrimination thresholds that were well matched with human psychophysical performance. Neural structures containing both excitatory and inhibitory connections were able to accurately simulate psychophysical thresholds for populations spanning a 20-fold increase in size (100-2000 units). More interestingly, equivalent levels of performance were also obtained using larger neural populations that contained *only* inhibitory connections.

Together with the model's robust performance as a function of the spread of excitatory connections ( $\sigma_E$ ), these results suggest that the sinusoidal trend in perceptual thresholds may be mediated primarily through signal enhancement associated with the strength ( $S_A$ ) and spread ( $\sigma_I$ ) of inhibitory connections within an anisotropic distribution of preferred motion patterns. The ability of preferred stimulus units to inhibit non-preferred units greatly reduced the level of noise across the population, thereby increasing discrimination. This helped offset the strong bias for expanding motions reported in the physiology and produced the cyclic trend in which radial discrimination thresholds were lowest.

Complimentary support for such inhibitory structures can be found in the performance of neural populations whose responses were thresholded prior to decoding the motion pattern estimate (Simulation 3). As with the various interconnected architectures examined here, such populations were able to accurately approximate human performance using as few as 500 units.

Although this strategy for reducing noise is computationally appealing, the simulations suggest that to be effective it would require a relatively high threshold ( $T_R \approx 35$  spikes/s). At this level, much of the visual motion information encoded across the population would be sacrificed to extract the perceptually relevant information. Such an effect cannot be easily reconciled with the correlations reported between perceptual performance and single cell responses in visual motion areas such as MT and MST (Britten et al., 1992; Celebrini & Newsome, 1994). Together with the necessity of *a priori* knowledge regarding what constitutes noise vs. signal implicit in this

structure, the use of such a mechanism in the perceptual task presented here seems unlikely.

However, the similarities between the sparse neural representation and a winner-take-all strategy for encoding motion pattern stimuli does provide some computational insights. In biologically plausible neural structures, winner-take-all strategies are often implemented using mutually inhibiting horizontal connections that suppress all but the strongest neural responses. Taken in the less extreme case of a winner-take-all strategy across neural sub-populations (i.e. contraction preferred units etc.), the resultant inhibitory structures would be qualitatively similar to the mutually inhibiting connection profiles explicitly simulated here.

### 4.3 Inhibitory Influences in MST

In the work presented here we have proposed a specific set of local interactions within a population MSTd-like units whose visual motion properties are consistent with the available physiological evidence. Specifically the model predicts an 80-100° spread of inhibition ( $\sigma_I$ ), as defined in the 2-D motion pattern space, whose profile is continuous across preferred motions. While such structures have not been explicitly examined in higher visual motion areas, such as MSTd, there is anecdotal support for the presence of inhibitory connections within the neurophysiological literature. Several studies have reported inhibitory effects in the motion pattern responses of MSTd neurons, although the degree and specificity of inhibition has not been characterized in detail (Duffy & Wurtz, 1991b; Lappe, et al., 1996).

Multi-cellular studies in MST would be well suited to examine this result in greater detail and further quantify the extent of inhibitory influence across motion pattern sensitive cells. By correlating neural responses across cell pairs as a function of the relative distances between their preferred motions and the retinotopic positions of their receptive field centers, multi-cellular studies could be used to quantify a) the spread of inhibition as a function of preferred motion patterns, b) the extent to which horizontal interactions span a continuous profile of relative strength and c) the retinotopic extent of such interactions.

It is worth noting that while the performance of the neural models suggests the presence of specific inhibitory connections between motion pattern detectors, the inhibitory effects implied by the model *do not* require the massive degree of interconnections implemented here. Equivalent interactions could be achieved in more biologically plausible architectures containing small populations of inhibiting interneurons whose pre-synaptic inhibition of preferred motion sub-populations follows an anti-hebbian rule of

connection strength. Discrete inhibitory profiles whose strength is constant within sub-populations could also be implemented without seriously degrading the visual motion information stored across the population. For equivalent representations of  $\sigma_1$  and/or half-width in continuous and discrete profiles respectively, the influence of the anti-preferred inhibitory structures would likely be similar such that discrimination thresholds continued to be well matched to human perceptual performance.

#### **4.4 Neural Interactions within and Across Visual Motion Areas**

The gross increase in computational complexity observed along the visual motion pathway has typically been associated with a feed-forward pooling of visual motion information *between* visual areas. In this scheme, neural responses to simple visual motion components are combined to encode more complex and perceptually relevant properties of the visual scene.

The model presented here does not explicitly preclude the existence of inhibitory feed-forward structures in the projection of motion information from MT to MSTd. While it is possible to obtain similar computational results using feed-forward mechanisms that inhibit “global” motion pattern responses via convergent “local” motion inputs, the mechanisms underlying the development of such a system remain unclear. In a previous computational model (Beardsley & Vaina, 1998; Beardsley et al., 2003) we illustrated the development of horizontal inhibition between MSTd-like units under a supervised learning rule. We also reported evidence of inhibitory feed-forward projections whose development appeared to be linked to the underlying learning rule. It seems likely that the visual motion pathway contains a combination of both inhibitory feed-forward and horizontal connections that act to maintain the visual information encoded across neural populations. Future extensions of this model to include a feed-forward layer of direction selective MT inputs and neurophysiological studies by others incorporating multi-cellular recording techniques within and across visual motion areas will likely provide the insights necessary to address these issues in greater detail.

#### **4.5 Relation to Existing Models of MSTd and Heading**

As we alluded to in the introduction, numerous biologically constrained feed-forward models of visual motion pooling from MT to MSTd have been developed to extract perceptually relevant visual motion properties. Three in

particular, Perrone & Stone (1994, 1998), Zemel & Sejnowski (1998), and Lappe et al. (1996), contain many of the underlying visual motion properties assumed here and could, in principle, also be used to model GMP performance. In practice, the methods employed in each model may in some ways restrict their extension to graded motion pattern discriminations, but in doing so they are likely to provide useful insights into the computational and structural requirements of higher-dimensional encoding and ‘perceptual’ decoding across multiple visual motion tasks.

In the template model of heading estimation proposed by Perrone and Stone (1994, 1998), perceptual estimates are obtained according to the gaze-stabilized translation properties of the most active template unit. In this case much of the visual motion information encoded across the population is discarded, removing a potential source of correlated signal that could be used to compensate the effects of internal and/or external noise. While such methods also have the advantage of removing much of the population noise, the trade-off in perceptual performance is strongly dependent on the underlying computational structure and physiological properties. As a result it is unclear how ‘perceptual’ performance for small perturbations in the overall motion would degrade as a function of neural and visual motion noise. Specifically, can maximal unit responses accurately decode the percept under noisy conditions or is it necessary to make more explicit use of the visual signal encoded across the population as a whole?

Other models, including Zemel & Sejnowski (1998) and Lappe et al. (Lappe & Rauschecker, 1993, 1995; Lappe et al., 1996; Lappe & Duffy, 1999), have decoded ‘perceptual’ estimates of heading based on the maximal activity obtained across neural sub-populations. While the signal integration afforded such methods is likely to provide a computationally more robust ‘perceptual’ estimate under noisy conditions, in the case of the GMP task it is not immediately clear how many neural sub-populations might be required, nor how many units each should contain.

Together with the extension of the model presented here to include a feed-forward layer of MT projections, these models could be readily extended to examine GMP discrimination across a wide range of stimulus conditions. In doing so each would provide additional insight into the relative roles of feed-forward versus horizontal connections and the range of decoding schemes sufficient to obtain equivalent measures of human perceptual performance. Specifically, to what extent might inhibitory feed-forward projections be used to mediate the decoded motion patterns? And what limitations do existing decoding strategies place on the extraction of equivalent measures of perceptual performance in the presence of noise (internal and external) and across multi-dimensional parameter spaces associated with dispirit perceptual tasks (e.g., Heading vs. GMP discrimination)?

## 5 SUMMARY

Within the visual cortex, the use of experimental and computational techniques to investigate neural connectivity continues to refine the role of intrinsic horizontal connections in the emergent computational and perceptual properties of the visual system. The model we have presented here builds on and extends these concepts to cortical areas later in the visual motion pathway. Through simulated populations of MSTd-like units we have identified a set of anti-preferred inhibitory structures whose computational effects on the encoded visual motion information are well matched to equivalent measures of human psychophysical performance. These structures are qualitatively similar to the inhibition of anti-preferred direction tuned cells reported in earlier visual motion areas such as MT and suggest a more a complex neural architecture throughout the visual motion system.

## ACKNOWLEDGMENTS

The authors wish to thank Colin Clifford and Peter Foldiak for their helpful suggestions during the early stages of this work. This work was supported by National Institutes of Health grant EY-2R01-07861-13 to LMV.

## REFERENCES

- Adini, Y., Sagi, D., & Tsodyks, M. (1997). Excitatory-inhibitory network in the visual cortex: Psychophysical evidence. *Proc. Natl. Acad. Sci.*, *94*, 10426-10431.
- Amir, Y., Harel, M., & Malach, R. (1993). Cortical hierarchy reflected in the organization of intrinsic connections in macaque monkey visual cortex. *J. Comp. Neurology*, *334*, 19-46.
- Andersen, R. A. (1997). Neural mechanisms of visual motion perception in primates. *Neuron*, *18*, 865-872.
- Andersen, R. A., Shenoy, K. V., Crowell, J. A., & Bradley, D. C. (2000). Neural Mechanisms for Self-Motion Perception in Area MST. In: M. Lappe (Ed.). *Neuronal Processing of Optic Flow*, 44 (pp. 219-234). New York: Academic Press.
- Ball, K., & Sekuler, R. (1987). Direction-specific improvement in motion discrimination. *Vision Res.*, *27* (6), 953-965.
- Beardsley, S. A., & Vaina, L. M. (1998). Computational modeling of optic flow selectivity in MSTd neurons. *Network: Comput. Neural Syst.*, *9*, 467-493.
- Beardsley, S. A., & Vaina, L. M. (2001). A laterally interconnected neural architecture in MST accounts for psychophysical discrimination of complex motion patterns. *J. Comput. Neurosci.*, *10*, 255-280.

- Beardsley, S. A., Ward, R. L., & Vaina, L. M. (2003). A feed-forward network model of spiral-planar tuning in MSTd. *Vision Res.*, *43*, 577-595.
- Ben-Yishai, B., Bar-Or, R. L., & Sompolinsky, H. (1995). Theory of orientation tuning in visual cortex. *Proc. Natl. Acad. Sci.*, *92*, 3844-3848.
- Bevington, P. (1969). *Data Reduction and Error Analysis for the Physical Sciences*, (p. 336). New York: McGraw-Hill.
- Boussaoud, D., Ungerleider, L. G., & Desimone, R. (1990). Pathways for motion analysis: cortical connections of the medial superior temporal and fundus of the superior temporal visual areas in the macaque. *J. Comp. Neurol.*, *296* (3), 462-495.
- Bremmer, F., Duhamel, J.-R., Ben Hamed, S., & Werner, G. (2000). Stages of Self-Motion Processing in Primate Posterior Parietal Cortex. In: M. Lappe (Ed.) *Neuronal Processing of Optic Flow*, 44 (pp. 173-198). New York: Academic Press.
- Britten, K. H., Newsome, W. T., Shadlen, M. N., Celebrini, S., & Movshon, J. A. (1996). A relationship between behavioral choice and the visual responses of neurons in macaque MT. *Vis. Neurosci.*, *13* (1), 87-100.
- Britten, K. H., Shadlen, M. N., Newsome, W. T., & Movshon, J. A. (1992). The analysis of visual motion: a comparison of neuronal and psychophysical performance. *J. Neurosci.*, *12* (12), 4745-4765.
- Britten, K. H., & van Wezel, R. J. A. (1998). Electrical microstimulation of cortical area MST biases heading perception in monkeys. *Nat. Neurosci.*, *1*, 59-63.
- Burr, D. C., Morrone, M. C., & Vaina, L. M. (1998). Large receptive fields for optic flow detection in humans. *Vision Res.*, *38* (12), 1731-1743.
- Carandini, M., & Ringach, D. L. (1997). Prediction of a recurrent model of orientation selectivity. *Vision Res.*, *37*, 3061-3071.
- Celebrini, S., & Newsome, W. T. (1994). Neuronal and psychophysical sensitivity to motion signals in extrastriate area MST of the macaque monkey. *J. Neurosci.*, *14* (7), 4109-4124.
- Celebrini, S., & Newsome, W. T. (1995). Microstimulation of extrastriate area MST influences performance on a direction discrimination task. *J. Neurophysiol.*, *73* (2), 437-448.
- Chey, J., Grossberg, S., & Mingolla, E. (1998). Neural dynamics of motion processing and speed discrimination. *Vision Res.*, *38*, 2769-2786.
- Coletta, N. J., Segu, P., & Tiana, C. L. (1993). An oblique effect in parafoveal motion perception. *Vision Res.*, *33* (18), 2747-2756.
- de Jong, B. M., Shipp, S., Skidmore, B., Frackowiak, R. S. J., & Zeki, S. (1994). The cerebral activity related to the visual perception of forward motion in depth. *Brain*, *117*, 1039-1054.
- deCharms, R. C., & Zador, A. (2000). Neural representation and the cortical code. *Annu. Rev. Neurosci.*, (23), 613-647.
- DeYoe, E. A., & Van Essen, D. C. (1988). Concurrent processing streams in monkey visual cortex. *Trends Neurosci.*, *11* (5), 219-226.
- Duffy, C. J. (2000). Optic Flow Analysis for Self-Movement Perception. In: M. Lappe (Ed.) *Neuronal Processing of Optic Flow*, 44 (pp. 199-218). New York: Academic Press.

- Duffy, C. J., & Wurtz, R. H. (1991a). Sensitivity of MST neurons to optic flow stimuli. I. A continuum of response selectivity to large-field stimuli. *J. Neurophysiol.*, *65* (6), 1329-1345.
- Duffy, C. J., & Wurtz, R. H. (1991b). Sensitivity of MST neurons to optic flow stimuli. II. Mechanisms of response selectivity revealed by small field stimuli. *J. Neurophysiol.*, *65* (6), 1346-1359.
- Duffy, C. J., & Wurtz, R. H. (1995). Response of monkey MST neurons to optic flow stimuli with shifted centers of motion. *J. Neurosci.*, *15* (7), 5192-5208.
- Duffy, C. J., & Wurtz, R. H. (1997a). Medial superior temporal area neurons respond to speed patterns in optic flow. *J. Neurosci.*, *17* (8), 2839-2851.
- Duffy, C. J., & Wurtz, R. H. (1997b). Planar directional contributions to optic flow responses in MST neurons. *J. Neurophysiol.*, *77*, 782-796.
- Edelman, S. (1996). Why Have Lateral Connections in the Visual Cortex? In: J. Sirosh, R. Miikkulainen, & Y. Choe (Eds.), *Lateral Interactions in the Cortex: Structure and Function*, Electronic Book (<http://www.cs.utexas.edu/users/nn/web-pubs/htmlbook96/edelman/>). Austin: The UTCS Neural Networks Research Group.
- Edwards, M., & Badcock, D. R. (1993). Asymmetries in the sensitivity to motion in depth: a centripetal bias. *Perception*, *22*, 1013-1023.
- Felleman, D. J., & Van Essen, D. C. (1991). Distributed hierarchical processing in the primate cerebral cortex. *Cereb. Cortex*, *1*, 1-47.
- Foldiak, P. (1993). The 'Ideal Homunculus': Statistical Inference from Neural Population Responses. In: F.H. Eeckman, & J.M. Bower (Eds.), *Computation and Neural Systems* (pp. 55-60). Norwell: Kluwer Academic Publishers.
- Freeman, T. C., & Harris, M. G. (1992). Human sensitivity to expanding and rotating motion: Effects of complementary masking and directional structure. *Vision Res.*, *32* (1), 81-87.
- Geesaman, B. J., & Andersen, R. A. (1996). The analysis of complex motion patterns by form/cue invariant MSTd neurons. *J. Neurosci.*, *16* (15), 4716-4732.
- Georgopoulos, A. P., Kettner, R. E., & Schwartz, A. B. (1988). Primate motor cortex and free arm movements to visual targets in three-dimensional space. II. Coding of the direction of movement by a neuronal population. *J. Neurosci.*, *8* (8), 2928-2937.
- Georgopoulos, A. P., Schwartz, A. B., & Kettner, R. E. (1986). Neuronal population coding of movement direction. *Science*, *233* (26), 1416-1419.
- Gibson, J. J. (1950). *The Perception of the Visual World*. (Boston: Houghton Mifflin).
- Gilbert, C., Das, A., Ito, M., Kapadia, M., & Westheimer, G. (1996). Spatial integration and cortical dynamics. *Proc. Natl. Acad. Sci. USA*, *93*, 615-622.
- Gilbert, C., & Wiesel, T. (1989). Columnar specificity of intrinsic horizontal and corticocortical connections in cat visual cortex. *J. Neurosci.*, *9* (7), 2432-2442.
- Gilbert, C. D. (1983). Microcircuitry of the visual cortex. *Ann. Rev. Neurosci.*, *6*, 217-247.
- Gilbert, C. D. (1985). Horizontal integration in the neocortex. *Trends Neurosci.*, (April), 160-165.
- Gilbert, C. D. (1992). Horizontal integration and cortical dynamics. *Neuron*, *9*, 1-13.

- Gilbert, C. D., & Wiesel, T. N. (1985). Intrinsic connectivity and receptive field properties in visual cortex. *Vision Res.*, *25* (3), 365-374.
- Graziano, M. S., Anderson, R. A., & Snowden, R. (1994). Tuning of MST neurons to spiral motions. *J. Neurosci.*, *14* (1), 54-67.
- Greenlee, M. W. (2000). Human cortical areas underlying the perception of optic flow: brain imaging studies. *Int. Rev. Neurobiol.*, *44*, 269-292.
- Grinvald, A., Lieke, E., Frostig, R. D., Gilbert, C. D., & Wiesel, T. N. (1986). Functional architecture of cortex revealed by optical imaging of intrinsic signals. *Nature*, *324*, 361-364.
- Gros, B. L., Blake, R., & Hiris, E. (1998). Anisotropies in visual motion perception: a fresh look. *J. Opt. Soc. Am. A*, *15* (8), 2003-2011.
- Grossberg, S., Mignolla, E., & Pack, C. (1999). A neural model of motion processing and visual navigation by cortical area MST. *Cereb. Cortex*, *9* (8), 878-895.
- Grossberg, S., & Williamson, J. R. (2001). A neural model of how horizontal and interlaminar connections of visual cortex develop into adult circuits that carry out perceptual grouping and learning. *Cereb. Cortex*, *11*, 37-58.
- Hatsopoulos, N., & Warren, W. J. (1991). Visual navigation with a neural network. *Neural Netw.*, *4*, 303-317.
- Haykin, S. (1999). *Neural Networks: A Comprehensive Foundation*, (p. 842). Upper Saddle River, NJ: Prentice Hall.
- Heeger, D. J. (1999). Linking visual perception with human brain activity. *Curr. Opin. Neurobiol.*, *9* (4), 474-479.
- Hertz, J., Krogh, A., & Palmer, R. G. (1991). Introduction to the Theory of Neural Computation. *A Lecture Notes Volume in the Santa Fe Institute Studies in the Sciences of Complexity* (p. 327). New York: Addison-Wesley Publishing Company.
- Kalaska, J. F., Caminiti, R., & Georgopoulos, A. P. (1983). Cortical mechanisms related to the direction of two-dimensional arm movements: relations in parietal area 5 and comparison with motor cortex. *Exp. Brain Res.*, *51*, 247-260.
- Kisvarday, Z., Toth, E., Rausch, M., & Eysel, U. (1997). Orientation-specific relationship between populations of excitatory and inhibitory lateral connections in the visual cortex of the cat. *Cereb. Cortex*, *7* (7), 605-618.
- Koehler, E., Anton, J., & Burnod, Y. (1999). Bayesian interference in populations of cortical neurons: A model of motion integration and segmentation in area MT. *Biol. Cybern.*, *80*, 25-44.
- Lagae, L., Maes, H., Raiguel, S., Xiao, D.-K., & Orban, G. A. (1994). Responses of macaque STS neurons to optic flow components: a comparison of areas MT and MST. *J. Neurophysiol.*, *71* (5), 1597-1626.
- Lappe, M. (2000). Computational mechanisms for optic flow analysis in primate cortex. In: M. Lappe (Ed.) *Neuronal Processing of Optic Flow*, 44 (pp. 235-268). New York: Academic Press.
- Lappe, M., Bremmer, F., Pökel, M., Thiele, A., & Hoffmann, K. (1996). Optic flow processing in monkey STS: A theoretical and experimental approach. *J. Neurosci.*, *16* (19), 6265-6285.

- Lappe, M., Bremmer, F., & van den Berg, A. V. (1999). Perception of self-motion from visual flow. *Trends Cogn. Sci.*, 3 (9), 329-336.
- Lappe, M., & Duffy, C. (1999). Optic flow illusion and single neuron behavior reconciled by a population model. *Eur. J. Neurosci.*, 11, 2323-2331.
- Lappe, M., & Rauschecker, J. P. (1993). A neural network for the processing of optic flow from ego-motion in man and higher mammals. *Neural Comput.*, 5, 374-391.
- Lappe, M., & Rauschecker, J. P. (1995). Motion anisotropies and heading detection. *Biol. Cybern.*, 72 (3), 261-277.
- Liu, L., & Hulle, V. (1998). Modeling the surround of MT cells and their selectivity for surface orientation in depth specified by motion. *Neural Comput.*, 10, 295-312.
- Lukashin, A. V., & Georgopoulos, A. P. (1993). A dynamical neural network model for motor cortical activity during movement: population coding of movement trajectories. *Biol. Cybern.*, 69, 517-524.
- Lukashin, A. V., & Georgopoulos, A. P. (1994). A neural network for coding of trajectories by time series of neuronal population vectors. *Neural Comput.*, 6, 19-28.
- Lukashin, A. V., Wilcox, G. L., & Georgopoulos, A. P. (1996). Modeling of directional operations in the motor cortex: a noisy network of spiking neurons is trained to generate a neural-vector trajectory. *Neural Netw.*, 9 (3), 397-410.
- Lund, J., Yoshioka, T., & Levitt, J. (1993). Comparison of intrinsic connectivity in different areas of the macaque monkey cerebral cortex. *Cereb. Cortex*, 3 (2), 148-162.
- Malach, R., Schirman, T., Harel, M., Tootell, R., & Malonek, D. (1997). Organization of intrinsic connections in owl monkey area MT. *Cereb. Cortex*, 7 (4), 386-393.
- Matthews, N., & Qian, N. (1999). Axis-of-motion affects direction discrimination, not speed discrimination. *Vision Res.*, 39, 2205-2211.
- Matthews, N., & Welch, L. (1997). Velocity-dependent improvements in single-dot direction discrimination. *Percept. Psychophys.*, 59 (1), 60-72.
- Maunsell, J. H., & Van Essen, D. C. (1983). The connections of the middle temporal visual area (MT) and their relationship to a cortical hierarchy in the macaque monkey. *J. Neurosci.*, 3 (12), 2563-2586.
- McGuire, B., Gilbert, C., Rivlin, P., & Wiesel, T. (1991). Targets of horizontal connections in macaque primary visual cortex. *J. Comp. Neurol.*, 305, 370-392.
- Meese, T., & Harris, M. (2001a). Independent detectors for expansion and rotation, and for orthogonal components of deformation. *Perception*, 30, 1189-1202.
- Meese, T. S., & Harris, M. G. (2001b). Broad direction bandwidths for complex motion mechanisms. *Vision Res*, 41 (15), 1901-1914.
- Meese, T. S., & Harris, S. J. (2002). Spiral mechanisms are required to account for summation of complex motion components. *Vision Res.*, 42, 1073-1080.
- Miikkulainen, R., & Sirosh, J. (1996). Introduction: The Emerging Understanding of Lateral Interactions in the Cortex. In: J. Sirosh, R. Miikkulainen, & Y. Choe (Eds.), *Lateral Interactions in the Cortex: Structure and Function*, Electronic Book (<http://www.cs.utexas.edu/users/nn/web-pubs/htmlbook96/miikkulainen/>). Austin: The UTCS Neural Networks Research Group.

- Morrone, C., Burr, D., & Vaina, L. (1995). Two stages of visual processing for radial and circular motion. *Nature*, *376*, 507-509.
- Morrone, M. C., Burr, D. C., Di Pietro, S., & Stefanelli, M. A. (1999). Cardinal directions for visual optic flow. *Curr. Biol.*, *9*, 763-766.
- Morrone, M. C., Tosetti, M., Montanaro, D., Fiorentini, A., Cioni, G., & Burr, D. C. (2000). A cortical area that responds specifically to optic flow, revealed by fMRI. *Nat. Neurosci.*, *3* (12), 1322-1328.
- Nowlan, S. J., & Sejnowski, T. J. (1995). A selection model for motion processing in area MT of primates. *J. Neurosci.*, *15* (2), 1195-1214.
- Oram, M. W., Foldiak, P., Perrett, D. I., & Sengpiel, F. (1998). The 'ideal homunculus': decoding neural population signals. *Trends Neurosci.*, *21* (8), 365-371.
- Orban, G. A., Lagae, L., Raiguel, S., Xiao, D., & Maes, H. (1995). The speed tuning of medial superior temporal (MST) cell responses to optic-flow components. *Perception*, *24* (3), 269-285.
- Orban, G. A., Lagae, L., Verri, A., Raiguel, S., Xiao, D., Maes, H., & Torre, V. (1992). First-order analysis of optical flow in monkey brain. *Proc. Natl. Acad. Sci. USA*, *89*, 2595-2599.
- Perrone, J., & Stone, L. (1994). A model of self-motion estimation within primate extrastriate visual cortex. *Vision Res.*, *34* (21), 2917-2938.
- Perrone, J. A., & Stone, L. S. (1998). Emulating the visual receptive-field properties of MST neurons with a template model of heading estimation. *J. Neurosci.*, *18* (15), 5958-5975.
- Pitts, R. I., Sundareswaran, V., & Vaina, L. M. (1997). A model of position-invariant, optic flow pattern-selective cells. In: *Computational Neuroscience: Trends in Research 1997* (pp. 171-176). New York: Plenum Publishing Corporation.
- Pouget, A., Zhang, K., Deneve, S., & Latham, P. E. (1998). Statistically efficient estimation using population coding. *Neural Comput.*, *10*, 373-401.
- Raymond, J. E. (1994). Directional anisotropy of motion sensitivity across the visual field. *Vision Res.*, *34* (8), 1029-1039.
- Rees, G., Friston, K., & Koch, C. (2000). A direct quantitative relationship between the function properties of human and macaque V5. *Nat. Neurosci.*, *3* (7), 716-723.
- Regan, D., & Beverley, K. (1978). Looming detectors in the human visual pathway. *Vision Res.*, *18*, 415-421.
- Regan, D., & Beverley, K. I. (1979). Visually guided locomotion: Psychophysical evidence for a neural mechanism sensitive to flow patterns. *Science*, *205*, 311-313.
- Royden, C. S. (1997). Mathematical analysis of motion-opponent mechanisms used in the determination of heading and depth. *J. Opt. Soc. Am. A*, *14*, 2128-2143.
- Rutschmann, R. M., Schrauf, M., & Greenlee, M. W. (2000). Brain activation during dichoptic presentation of optic flow stimuli. *Exp. Brain Res.*, *134*, 533-537.
- Saito, H.-a., Yukie, M., Tanaka, K., Hikosaka, K., Fukada, Y., & Iwai, E. (1986). Integration of direction signals of image motion in the superior temporal sulcus of the macaque monkey. *J. Neurosci.*, *6* (1), 145-157.

- Sakai, K., & Miyashita, Y. (1991). Neural organization for the long-term memory of paired associates. *Nature*, *354*, 152-155.
- Salinas, E., & Abbott, L. (1994). Vector reconstruction from firing rates. *J. Comput. Neurosci.*, *1*, 89-107.
- Salinas, E., & Abbott, L. (1995). Transfer of coded information from sensory to motor networks. *J. Neurosci.*, *15*, 6461-6474.
- Salzman, C. D., Britten, K. H., & Newsome, W. T. (1990). Cortical microstimulation influences perceptual judgements of motion direction. *Nature*, *346*, 174-177.
- Salzman, C. D., Murasugi, C. M., Britten, K., & Newsome, W. T. (1992). Microstimulation in visual area MT: effects on direction discrimination performance. *J. Neurosci.*, *12* (6), 2331-2355.
- Sanger, T. D. (1996). Probability density estimation for the interpretation of neural population codes. *J. Neurophysiol.*, *76* (4), 2790-2793.
- Schaafsma, S. J., & Duysens, J. (1996). Neurons in the ventral intraparietal area of awake macaque monkey closely resemble neurons in the dorsal part of the medial superior temporal area in their responses to optic flow patterns. *J. Neurophysiol.*, *76* (6), 4056-4068.
- Schwartz, A. B., Kettner, R. E., & Georgopoulos, A. P. (1988). Primate motor cortex and free arm movements to visual targets in three-dimensional space. I. Relations between single cell discharge and direction of movement. *J. Neurosci.*, *8* (8), 2913-2827.
- Seung, H. S., & Sompolinsky, H. (1993). Simple models for reading neuronal population codes. *Proc. Natl. Acad. Sci. USA*, *90*, 10749-10753.
- Shadlen, M., & Newsome, W. (1998). The variable discharge of cortical neurons: implications for connectivity, computation, and information coding. *J. Neurosci.*, *18* (10), 3870-3896.
- Shadlen, M. N., & Newsome, W. T. (1994). Noise, neural codes, and cortical organization. *Curr. Opin. Neurobiol.*, *4*, 569-579.
- Siegel, R. M., & Read, H. L. (1997). Analysis of optic flow in the monkey parietal area 7a. *Cereb. Cortex*, *7* (4), 327-346.
- Snippe, H. (1996). Parameter extraction from population codes: A critical assessment. *Neural Comput.*, *8*, 511-530.
- Snowden, R. J., & Milne, A. B. (1996). The effects of adapting to complex motions: position invariance and tuning to spiral motions. *J. Cognit. Neurosci.*, *8* (4), 412-429.
- Snowden, R. J., & Milne, A. B. (1997). Phantom motion aftereffects - evidence of detectors for the analysis of optic flow. *Curr. Biol.*, *7*, 717-722.
- Softky, W. (1995). Simple codes versus efficient codes. *Curr. Opin. Neurobiol.*, *5*, 239-247.
- Softky, W., & Koch, C. (1993). The highly irregular firing of cortical cells is inconsistent with temporal integration of random EPSPs. *J. Neurosci.*, *13* (1), 334-350.
- Stemmler, M., Usher, M., & Niebur, E. (1995). Lateral interactions in primary visual cortex: A model bridging physiology and psychophysics. *Science*, *269*, 1877-1880.
- Sundareswaran, V., & Vaina, L. M. (1996). Adaptive computational models of fast learning of motion direction discrimination. *Biol. Cybern.*, *74*, 319-329.

- Tanaka, K., Fukada, Y., & Saito, H.-A. (1989). Underlying mechanisms of the response specificity of expansion/contraction and rotation cells in the dorsal part of the medial superior temporal area of the macaque monkey. *J. Neurophysiol.*, *62* (3), 642-656.
- Tanaka, K., & Saito, H.-A. (1989). Analysis of motion of the visual field by direction, expansion/contraction, and rotation cells clustered in the dorsal part of the medial superior temporal area of the macaque monkey. *J. Neurophysiol.*, *62* (3), 626-641.
- Taylor, J. G., & Alavi, F. N. (1996). A Basis for Long-Range Inhibition Across Cortex. In: J. Sirosh, R. Miikkulainen, & Y. Choe (Eds.), *Lateral Interactions in the Cortex: Structure and Function*, Electronic Book (<http://www.cs.utexas.edu/users/nn/web-pubs/htmlbook96/taylor/>). Austin: The UTCS Neural Networks Research Group.
- Te Pas, S. F., Kappers, A. M., & Koenderink, J. J. (1996). Detection of first-order structure in optic flow fields. *Vision Res.*, *36* (2), 259-270.
- Teich, A. F., & Qian, N. (2002). Learning and adaptation in a recurrent model of V1 orientation selectivity. *J. Neurophysiol.*, in press.
- Tootell, R. B. H., Reppas, J. B., Kwong, K. K., Malach, R., Born, R. T., Brady, T. J., Rosen, B. R., & Belliveau, J. W. (1995). Functional analysis of human MT and related visual cortical areas using magnetic resonance imaging. *J. Neurosci.*, *15* (4), 3215-3230.
- Ts'o, D., Gilbert, C. D., & Wiesel, T. N. (1986). Relationships between horizontal interactions and functional architecture in cat striate cortex as revealed by cross-correlation analysis. *J. Neurosci.*, *6* (4), 1160-1170.
- Vaina, L. M. (1998). Complex motion perception and its deficits. *Curr. Opin. Neurobiol.*, *8* (4), 494-502.
- Vaina, L. M., Solovyev, S., Kopicik, M., & Chowdhury, S. (2000). Impaired self-motion perception from optic flow: a psychophysical and fMRI study of a patient with a left occipital lobe lesion. *Soc. Neurosci. Abst.*, *26*, 1065.
- Vaina, L. M., Sundaeswaran, V., & Harris, J. G. (1995). Learning to ignore: psychophysics and computational modeling of fast learning of direction in noisy motion stimuli. *Cognit. Brain Res.*, *2* (3), 155-163.
- van den Berg, A. V. (2000). Human Ego-Motion Perception. In: M. Lappe (Ed.) *Neuronal Processing of Optic Flow*, 44 (pp. 3-25). New York: Academic Press.
- Van Essen, D. C., & Maunsell, J. H. R. (1983). Hierarchical organization and functional streams in the visual cortex. *Trends Neurosci.*, *6* (9), 370-375.
- Wang, R. (1995). A simple competitive account of some response properties of visual neurons in area MSTd. *Neural Comput.*, *7*, 290-306.
- Wang, R. (1996). A network model for the optic flow computation of the MST neurons. *Neural Netw.*, *9* (3), 411-426.
- Wiskott, L., & von der Malsburg, C. (1996). Face Recognition by Dynamic Link Matching. In: J. Sirosh, R. Miikkulainen, & Y. Choe (Eds.), *Lateral Interactions in the Cortex: Structure and Function*, Electronic Book (<http://www.cs.utexas.edu/users/nn/web-pubs/htmlbook96/wiskott/>). Austin: The UTCS Neural Networks Research Group.
- Worgotter, F., Niebur, E., & Christof, K. (1991). Isotropic connections generate functional asymmetrical behavior in visual cortical cells. *J. Neurophysiol.*, *66* (2), 444-459.

- Zemel, R., Dayan, P., & Pouget, A. (1998). Probabilistic interpretation of population codes. *Neural Comput.*, *10*, 403-430.
- Zemel, R. S., & Sejnowski, T. J. (1998). A model for encoding multiple object motions and self-motion in area MST of primate visual cortex. *J. Neurosci.*, *18* (1), 531-547.
- Zhang, K., Sereno, M. I., & Sereno, M. E. (1993). Emergence of position-independent detectors of sense of rotation and dilation with Hebbian learning: an analysis. *Neural Comput.*, *5*, 597-612.
- Zhao, L., Vaina, L. M., LeMay, M., Kader, B., Chou, I. S., & Kemper, T. (1995). Are there specific anatomical correlates of global motion perception in the human visual cortex? *Invest. Ophthalmol. Vis. Sci.*, *36* (4), S56.
- Zohary, E. (1992). Population coding of visual stimuli cortical neurons tuned to more than one dimension. *Biol. Cybern.*, *66*, 265-272.